Numerical Modeling of No Vent Filling of a Cryogenic Tank

Alok Majumdar[1], Andre LeClair[2]
Thermal Analysis Branch, NASA Marshall Space Center, Huntsville, AL 35812

Jason Hartwig[3]
Liquid Propulsion System Branch, NASA/Glenn Research Center, Cleveland, OH 44135

Adam Martin[4] & Noah Rhys[5]
Propulsion Research and Technology Branch, NASA Marshall Space Center, Huntsville, AL 35812

ABSTRACT

This paper presents a multi-node finite volume model of the chilling and filling of a cryogenic tank using the Generalized Fluid System Simulation Program (GFSSP), a general purpose flow network code. Vented Chill and No Vent Fill (VCNVF) tests were conducted at Marshall Space Flight Center where a flight-like tank was filled with liquid nitrogen from a supply tank. In the VCNVF tests, the tank was partially chilled while the vent valve was open. After the partial chilling, the vent valve was closed and the tank was filled without any venting. An integrated numerical model of the test set up was developed. The model included the transfer line from the supply tank, the target tank with the spray nozzle and solid walls, and the discharge line with the vent valve. The tank was discretized into multiple fluid nodes and branches to represent the ullage and liquid nitrogen and multiple solid nodes to represent the tank wall and structure. The heat transfer between solid to fluid was calculated from pool boiling correlations which include film, transition, and nucleate boiling, as well as natural convection during pre- and post-boiling. The model also accounts for the condensation of vapor in the tank when it comes in contact with the liquid spray. The predicted pressure, resident mass, wall and ullage temperature in the tank were compared with the test data.

Nomenclature

A = area

B = Laplace reference length [m] $\left(\sqrt{\frac{\sigma}{g\left(\rho_f - \rho_v\right)}} \right)$

C_p = specific heat
D = diameter
d = bubble diameter
g = gravitational acceleration
H = heat transfer coefficient
h = enthalpy
λ = latent heat of vaporization
k = thermal conductivity
J = Mechanical Equivalent of Heat (= 778 lb_f – ft/Btu)
K_f = flow resistance coefficient
L = characteristic length
M = molecular weight
m = resident mass
$\dot{m}$ = Mass flow rate

[1]Aerospace Technologist, Propulsion Systems Department, AIAA Senior Member.
[2] Aerospace Technologist, Propulsion Systems Department.
[3] Research Aerospace Engineer, Fluids and Cryogenics Branch, AIAA Associate Fellow
[4]
[5]

Nu = Nusselt number
p = pressure

Pr = Prandtl number $\left(\frac{\mu c_p}{k}\right)$

Gr = Grashof number $\left(\frac{g\beta\left(T_s - T_\infty\right)L^3}{\nu^2}\right)$

Ra = Rayleigh number $\left(\left(\frac{L^3\rho_v\left(\rho_l - \rho_v\right)g}{\mu_v{}^2}\right)\left(\frac{c_p\mu}{k}\right)_v\right)$

V = volume
Q, $\dot{q}$ = heating rate
q" = heat flux
T = temperature

Greek
α = thermal diffusivity
μ = viscosity
v = kinematic viscosity
ρ = density
σ = surface tension
Θ = angle between flow vector and gravity vector
Δτ = time step

Subscript
c = critical
CHF = critical heat flux
f = liquid
FB = film boiling
v = vapor
NB = nucleate boiling
NC = natural convection
LFP = Leidenfrost point
ONB = onset nucleate boiling
S = heater surface
i = node
ij = branch or conductor
t = turbulent
u = ullage
v = vapor

I. Introduction

Filling a cryogenic tank in deep space in the absence of gravity is challenging because in a non-stratified environment liquid propellant may not settle at the tank bottom as it does on earth. There is a strong possibility that liquid propellant may exit through the vent valve, which is typically located at the top of the tank to vent propellant vapor. To reduce the loss of precious propellant, a "charge-hold-vent" method of tank filling [1] was developed. During the charge cycle, a small quantity of liquid cryogen is injected into the evacuated tank. Initially, the liquid flashes due to the low tank pressure, and then the remaining liquid droplets evaporate as they contact warm hydrogen vapor or the tank wall.

During the hold period, the circulating flow pattern induced from the spray nozzles provides convective heat transfer from cold vapor to the tank wall. The primary mode of heat transfer during the hold is convection. At the completion of the hold period, the pressure has risen considerably and the tank is ready to be vented. Since venting occurs as an isentropic blowdown, some additional cooling may be recovered by stage-wise venting. This method, however, proves difficult to find an optimum frequency of "charge- hold-vent" cycles and the amount of charge for each cycle.

A simpler method is that of Vented-Chill / No-Vent-Fill (VCNVF) [2]. In this method, the tank's vent valve is open for an initial period while the tank walls are chilled with a spray of cryogenic liquid that boils to vapor and exits through the vent. When the tank walls have sufficiently chilled, the vent valve is closed and the tank is filled with liquid. Care must be taken with the timing of the vent closure. If the vent is closed too early, residual heat in the walls may drive sufficient boil-off to raise the tank pressure high enough to stall the inlet flow. If the vent is closed too late, some liquid propellant may be lost out the vent. Compared to the Charge-Hold-Vent method, VCNVF is less mass efficient; the gas being vented during the chill may not be extracting the maximum possible thermal energy from the tank wall. There is always the risk that some of the precious liquid propellant will be vented. However, VCNVF is much simpler from an operational standpoint. The transfer lines need to be chilled down just once and there is less cycling of inlet and vent valves. Since there is no hold period, overall loading time is likely to decrease.

In this paper, a numerical model of a VCNVF experiment is described. The modeling was performed using the Generalized Fluid System Simulation Program (GFSSP) [3]. GFSSP is a finite volume based network flow analysis code. GFSSP has previously been used [4] to model the loading of propellant in the External Tank of Space Shuttle and the "charge-hold-vent" process [5] described in Reference 1. Satisfactory comparison between test data and predictions was observed. In this paper, the experimental data of Reference 2 has been used to verify the modeling of Vented Chill and No Vent filling of a cryogenic tank.

II. Finite Volume Modeling of Tank Chill & Fill

In the Finite Volume Formulation [6], a thermo-fluid system is discretized into a finite number of nodes and branches to represent a flow network consisting of different flow components such as pipes, valves and orifices. Many thermo-fluid systems, including the chilling of a cryogenic tank, need to model solid to fluid (conjugate) heat transfer. In that situation, the solid wall in contact with the fluid is also discretized into solid nodes.

The mass and energy conservation equations are solved at the fluid nodes. The momentum conservation equations are solved at the flow branches. The energy conservation equations for the solid are solved at the solid nodes. The thermodynamic and thermo-physical properties required to construct the conservation equations are calculated using a thermodynamic property program that provides the properties of a real fluid for all possible states e,g. liquid, vapor, saturation, or super-critical.

Governing Equations

The GFSSP Users' Manual [3] provides a detailed description of all governing equations. This section provides a brief description of the conservation equations and other empirical correlations used in the development of the tank chill and fill model. Figure 1 displays a schematic showing adjacent nodes, their connecting branches, and the indexing system.

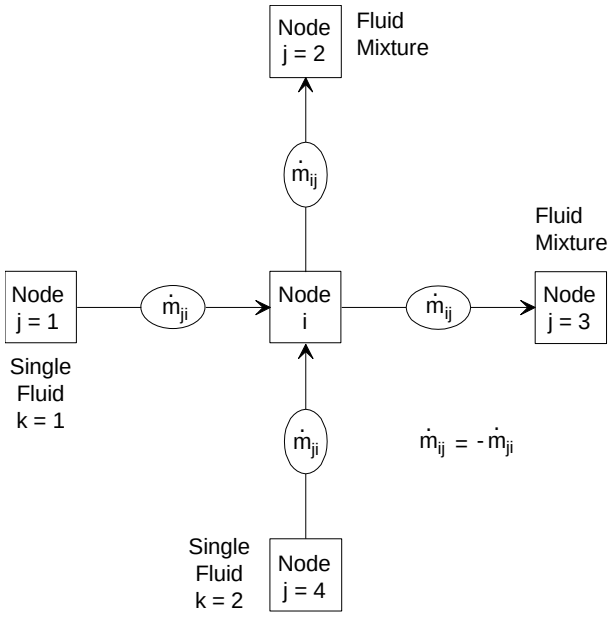

Figure 1 - Schematic of GFSSP Nodes, Branches and Indexing Practice

GFSSP calculates pressure from the mass conservation equation. The mass conservation equation for node i can be expressed as:

$$\frac{m_{\tau+\Delta\tau} - m_{\tau}}{\Delta\tau} = -\sum_{j=1}^{j=n} \dot{m}_{ij} \qquad (1)$$

Figure 2 shows the schematic of a Branch. It may be noted that the mass flow is driven by pressures which are located at the nodes (*i* and *j*). The gravity acts vertically downward. The angle between flowrate and gravity vector is θ.

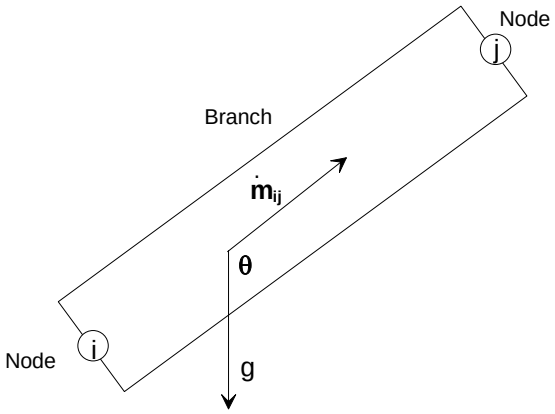

Figure 2 - Schematic of a Branch showing location of pressure, mass flowrate and gravity

GFSSP calculates flow rate from the momentum conservation equation which can be written as:

$$\left(p_i - p_j\right)A_{ij} + \frac{\rho g V Cos\theta}{g_c} - K_f \dot{m}_{ij}\left|\dot{m}_{ij}\right|A_{ij} = 0 \qquad (2)$$

The first term in Equation (2) is the pressure force applied on the fluid. The second term represents the gravitational force. It may be noted that at θ = 180° the fluid is flowing against gravity; at θ = 90° the fluid is flowing horizontally, and gravity has no effect on the flow. The third term represents the frictional effect. Friction was modeled as a product of K_f and the square of the flow rate and area. K_f is a function of the fluid density in the branch and the nature of the flow passage being modeled by the branch. The calculation of K_f for different types of flow passages is described in reference [3].

The energy conservation equation is expressed in terms of enthalpy which is solved at the nodes:

$$\frac{m\left(h-\frac{p}{\rho J}\right)_{\tau+\Delta\tau}-m\left(h-\frac{p}{\rho J}\right)_{\tau}}{\Delta\tau}=\sum_{j=1}^{j=n}\left\{MAX\left[-\dot{m}_{ij},0\right]h_j-MAX\left[\dot{m}_{ij},0\right]h_i\right\}+Q_i \qquad (3)$$

The left hand side of Equation (3) represents the rate of change of internal energy. The first term in the right hand side represents the net influx of energy due to advection. The MAX operator used in Equation 3 is known as an upwind differencing scheme and has been extensively employed in the numerical solution of Navier-Stokes equations in convective heat transfer and fluid flow applications [7]. When the flow direction is not known beforehand, this operator allows the transport of energy only from its upstream neighbor. In other words, the upstream neighbor influences its downstream neighbor but not vice versa. Q_i represents any external heat source.

The resident mass at the node is calculated from the equation of state which can be expressed as:

$$m=\frac{pV}{zRT} \qquad (4)$$

z is the compressibility factor of the fluid which is derived from thermodynamic properties. All thermodynamic and thermo-physical properties are calculated by the GASP computer code [8] from the calculated pressure and enthalpy at the nodes. It may be noted that equation (4) is valid for liquid, vapor, and liquid-vapor mixture.

For a two-phase mixture, z is computed from the following relation.

$$z=\frac{p}{\rho_{mix}RT} \qquad (5)$$

where $$\rho_{mix}=\frac{\rho_l\rho_g}{x\rho_l-(1-x)\rho_g} \qquad (6)$$

and, $$x=\frac{h-h_f}{h_g-h_f}. \qquad (7)$$

The energy conservation equation for the solid is solved at the solid node and is expressed as:

$$\frac{\partial}{\partial\tau}\left(mC_pT_s^i\right)=\sum_{j_f=1}^{n_{sf}}\dot{q}_{sf}+\dot{S}_i \qquad (8)$$

The left hand side of the equation represents the rate of change of energy. The first term in the right hand side represents convective heat transfer between fluid and solid node and is expressed in Equation (9):

$$\dot{q}_{sf}=H_{ij_f}A_{ij_f}\left(T_f^{j_f}-T_s^i\right) \qquad (9)$$

$\dot{S}_i$ represents any external heat source.

Numerical Solution

GFSSP numerically solves the governing equations to compute pressure, enthalpy, flowrate and other fluid properties in a given flow circuit. The mathematical closure is described in Table 1 where each variable and the designated governing equation to solve that variable are listed. It may be noted that the pressure is calculated from the mass conservation equation although pressure does not explicitly appear in equation 1. This is, however, possible in the iterative scheme where pressures are corrected to reduce the residual error in the mass conservation equation.

Table 1 – Mathematical Closure

Variable Number	Variable Name	Designated Equation to Solve the Variable
1	Pressure	Mass Conservation
2	Flowrate	Momentum Conservation
3	Fluid Enthalpy	Energy Conservation of Fluid
4	Solid Temperature	Energy Conservation of Solid
5	Fluid Mass	Thermodynamic State

There are two types of numerical methods available to solve a set of non-linear coupled algebraic equations: (1) the successive substitution method and (2) the Newton-Raphson method. In GFSSP, a combination of the successive substitution method and the Newton-Raphson method is used to solve the set of equations. This method is called SASS (Simultaneous Adjustment with Successive Substitution). In this scheme, the mass and momentum conservation equations are solved by the Newton-Raphson method. The energy and species conservation equations are solved by the successive substitution method. The underlying principle for making such a division was that the equations that are more strongly coupled are solved by the Newton-Raphson method. The equations that are not strongly coupled with the other set of equations are solved by the successive substitution method. Thus, the computer memory requirement can be significantly reduced while maintaining superior numerical convergence characteristics.

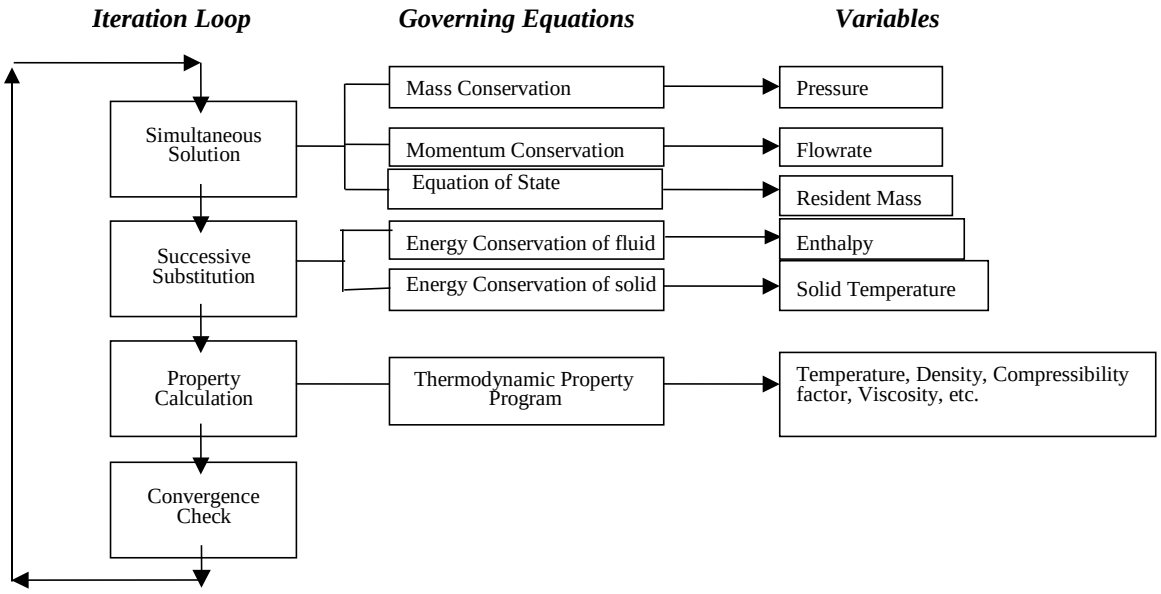

Figure 3. SASS (Simultaneous Adjustment with Successive Substitution) Scheme for solving Governing Equations

Pool Boiling Model

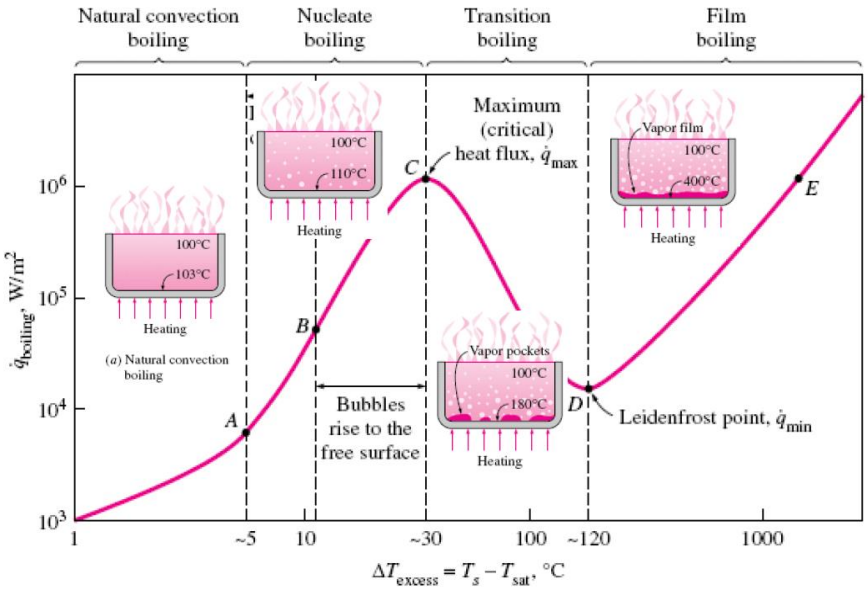

Figure 4. Heat Flux Distribution during Pool Boiling

The chilldown of a propellant tank is primarily governed by boiling of liquid propellant at the tank wall. Figure 4 shows different boiling regimes. During chilldown, the boiling curve moves from right to left (E - D - C – B – A). Initially, the temperature difference between the solid wall and saturation temperature is in the order of several hundred degrees. Therefore, the boiling starts in the Film Boiling regime and continues until it reaches the Leidenfrost point. After reaching the Leidenfrost point, it switches to Transition Boiling and continues to Critical Heat Flux. Nucleate Boiling starts after reaching Critical Heat Flux and, finally, heat transfer is controlled by natural convection beyond the Onset of Nucleate Boiling (ONB).

Hartwig [9] compiled a set of pool boiling correlations for all regimes to model the quenching mechanism for cryogenic fluids. The compilation includes correlations for normal and reduced gravity. The present paper uses the correlations for normal gravity to model the chilldown of the CRYOTE tank.

Film Boiling Correlation

The heat transfer coefficient during film boiling was evaluated from Wang's [10] correlation which can be expressed as:

$$H_{FB} = C\left(R\left(\frac{\lambda'}{c_{p,v}\Delta T}\right)\right)^m\left(\frac{k_v}{L_x}\right) \quad (10)$$

$$R = \left(\frac{L_x^3\rho_v(\rho_f-\rho_v)g}{\mu^2}\right)\left(\frac{c_{p,v}\mu}{k_v}\right) \quad (11)$$

For a spherical tank,

$$C = 0.15\,;\, m = 1/3\,;\, L_x = Tank\ Diameter$$

$$\lambda' = h_{fg} + 0.5c_{p,v}\Delta T \quad (12)$$

Leidenfrost Point

Leidenfrost point was calculated using the Baumeister [11] correlation which can be expressed as:

$$\Delta T_{LFP} = \frac{27}{32} T_C \left(1 - e^{-0.52\times 10^4 \left(\frac{\rho_S}{M_S}\right)^{1/3} \frac{1}{\sigma}}\right) - T_{sat} \quad (13)$$

Critical Heat Flux

The critical heat flux was calculated using Lienhard's [12] correlation which is expressed as:

$$q''_{CHF} = f\left(l'\right) \frac{\pi}{24} \rho_v^{1/2} h_{fg} \left(\sigma g \left(\rho_f - \rho_v\right)\right)^{1/4} \quad (14)$$

For a spherical tank, $f\left(l'\right) = 0.84$

Transition Boiling

The heat transfer coefficient during transition boiling is evaluated by logarithmic interpolation between the Leidenfrost and Critical Heat Flux points.

$$H_{TB} = e^{\left(\frac{\ln(H_{LFP}) - \ln(H_{CHF})}{\ln(\Delta T_{LFP}) - \ln(\Delta T_{CHF})} (\ln(\Delta T) - \ln(\Delta T_{CHF})) + \ln(H_{CHF})\right)} \quad (15)$$

Where

$$H_{CHF} = A_{CHF} \Delta T_{CHF}^{2.33} \quad (16)$$

$$A_{CHF} = \left(8.7 \times 10^{-4} \left(\frac{B}{h_{fg} \rho_v \nu_f}\right)^{0.7} \left(\frac{PB}{\sigma}\right)^{0.7} \left(\frac{k_f}{B}\right)\right)^{3.33} \quad (17)$$

Nucleate Boiling

The heat transfer coefficient is calculated from Minchenko's [13] correlation which can be expressed as:

$$H_{NB} = A_{NB} \Delta T^{2.33} \quad (18)$$

$$A_{NB} = \left(8.7 \times 10^{-4} \left(\frac{B}{h_{fg} \rho_v \nu_f}\right)^{0.7} \left(\frac{PB}{\sigma}\right)^{0.7} \left(\frac{k_f}{B}\right)\right)^{3.33} \quad (19)$$

Natural Convection

The heat transfer coefficient during natural convection was calculated using the correlation of Shirai [14]:

$$H_{NC} = 0.16 \frac{k_f}{L_c} \left(Pr_f Gr_f\right)^{1/3} \quad (20)$$

Onset of Nucleate Boiling (ONB)

ΔT_{ONB} is calculated by setting H_{NB} equal to H_{NC} and solving for ΔT:

$$\Delta T_{ONB} = \left(\frac{A_{NC}}{A_{NB}}\right)^{0.5} \quad (21)$$

$$A_{NC} = \frac{H_{NC}}{\Delta T^{1/3}} \quad (22)$$

Finally, once all the terms have been defined according to the equations above, the correct heat transfer coefficient has been assigned depending on the wall superheat using the following logic:

If $0 < \Delta T \leq \Delta T_{ONB}$

Use H_{NC}

Else if $\Delta T_{ONB} < \Delta T \leq \Delta T_{CHF}$

Use H_{NB}

Else if $\Delta T_{CHF} < \Delta T \leq \Delta T_{LFP}$

Use H_{TB}

Else if $\Delta T_{LFP} \leq \Delta T$

Use H_{FB}

Condensation Model

Some of the vapor in the tank ullage condenses during the process of filling the tank by spraying liquid propellant in the tank. Condensation of vapor occurs when saturated vapor comes in contact with subcooled liquid spray. Condensation reduces the tank pressure and therefore must be accounted in the numerical model to predict the pressure and the resident liquid mass in the tank. A simple condensation model has been developed for the present analysis.

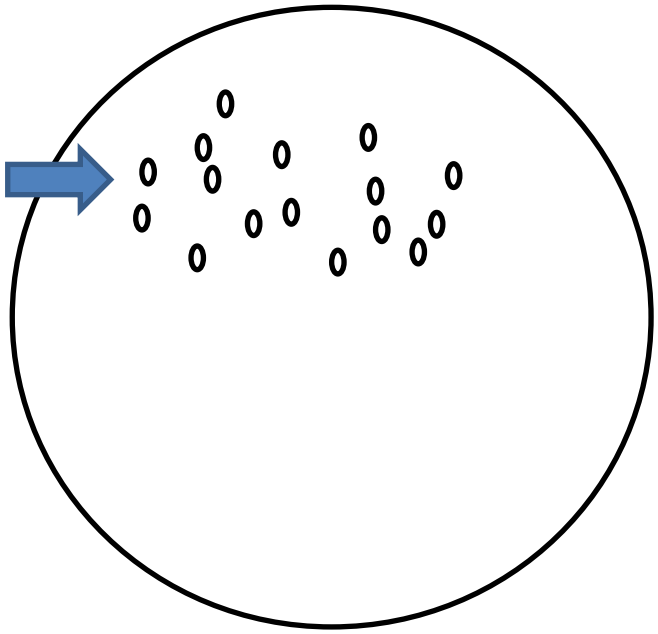

Figure 5. Schematic of Condensation Model

Figure 5 shows the schematic of condensation model. It has been assumed that the liquid spray in the tank remain in the form of droplets of constant diameter. The saturated vapor in contact with the liquid droplet rejects the latent heat of vaporization to condense. The number of droplets in the resident mass can be estimated from the resident mass:

$$N_i = \frac{\dot{m}_i \Delta\tau_{res}}{\frac{\pi d^3}{6}\rho_L} \quad (23)$$

Where $\Delta\tau = \frac{\Delta H}{V_i}$ (24)

ΔH is a characteristic length scale. In this analysis it was assumed to be 50% of node height.

The heat transfer from vapor to liquid can be calculated from the following expressions:

$$\dot{q} = HA(T_{sat} - T_L) \quad (25)$$

$$A = N_i \pi d^2 \quad (26)$$

$$H = \frac{k_L}{d} Nu_{D,in} \quad (27)$$

According to Kronig and Brink [15] $Nu_{D,in}$= 17.9. The bubble diameter was assumed to be 1 mm.

The condensation rate per unit volume can be expressed as:

$$\dot{m}''' = \frac{\dot{q}}{\lambda V} \quad (28)$$

III. Vented Chill and No Vent Fill (VCNVF) Experiments

This section briefly describes Vented-Chill / No-Vent Fill (VCNVF) experiments conducted at Marshall Space Flight Center using liquid nitrogen (LN2) to fill the CRYOTE (Cryogenic Testbed) tank. Figure 6 presents a side-view of the CRYOTE tank. Note that the centerline Thermodynamic Vent System (TVS) dip tube was not present for the VCNVF tests.

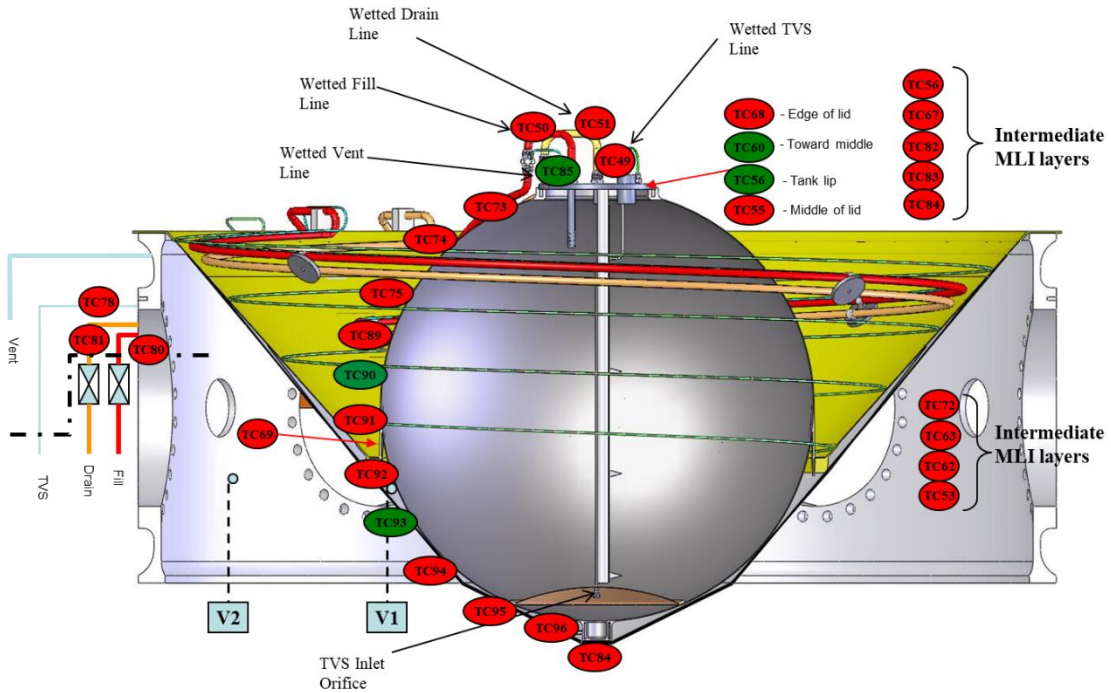

Figure 6: CRYOTE tank with Thermocouple Locations

The tank is a 6-4 Titanium sphere with outer diameter of 29.70 inches and 0.05 inch wall thickness. To minimize heat conduction into the tank, it is mounted in a cone-shaped composite skirt. Plumbing into and out of the tank passes through the stainless steel lid which has a diameter of 8.00 inches and 0.38 inch thickness. The mass of the titanium sphere is 22.7 lbm, and the stainless steel lid is 6.35 lbm.

Tests were carried out in a vacuum chamber. A larger tank, the Vibro-Acoustic Test Article (VATA), served as the supply tank. To minimize radiation heat transfer, CRYOTE was covered in multi-layer insulation (MLI). Based on earlier boil-off tests, steady-state heat leak into CRYOTE is estimated at 10 watts.

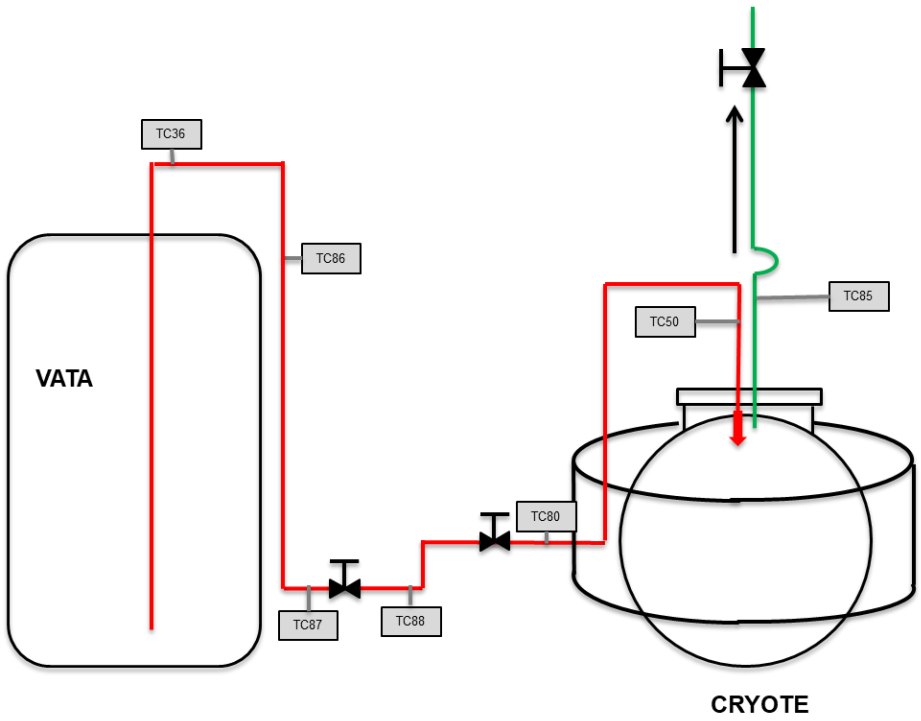

Figure 7: Transfer Line connecting VATA and CRYOTE tanks

Figure 7 presents the transfer line between the VATA supply tank and CRYOTE receiver tank. The transfer line is approximately 210 inches of 0.5-inch outer-diameter stainless steel tubing, with a mass of 4.2 lb. There is no separate pre-chill of the transfer line: vapor created during line chilldown enters the CRYOTE tank, from which it is then vented. A series of thermocouples measure the temperature of the outside wall of the pipe. TC50, located just upstream of the CRYOTE injector, is a wetted thermocouple on the inside wall of the transfer line. TC85, just downstream of the vent, is also a wetted thermocouple on the inside wall of the vent line.

Figure 6 presents the CRYOTE tank instrumentation. Most of the thermocouples are placed on the outside wall of the tank. A green oval indicates that the thermocouple was tested as a possible trigger for closure of the vent valve. Not shown are TC49 and TC79, wetted thermocouples inside the tank at the 39.5% and 95% fill levels.

In addition to temperature measurements, pressure transducers measure the pressures in the ullage of VATA and CRYOTE, as well as the pressure just upstream of the CRYOTE injector. Load cells provide the mass of CRYOTE. After the CRYOTE vent is closed, the change in tank mass over time can be used to estimate the transfer line flow rate; there was no flow meter used in the test.

CRYOTE tested three difference injectors in the test program; Figure 8 illustrates the three-spray nozzles, TF6, TF8, and TF10, which form one of the CRYOTE injectors tested, placed under the tank lid. They are ¼ inch spray nozzles with a 170 degree spray angle. Manufacturer's data indicate an approximate 1:2:3 ratio in flow rate, so that roughly 1/3 of the inlet flow will be directed upwards, and 2/3 downwards.

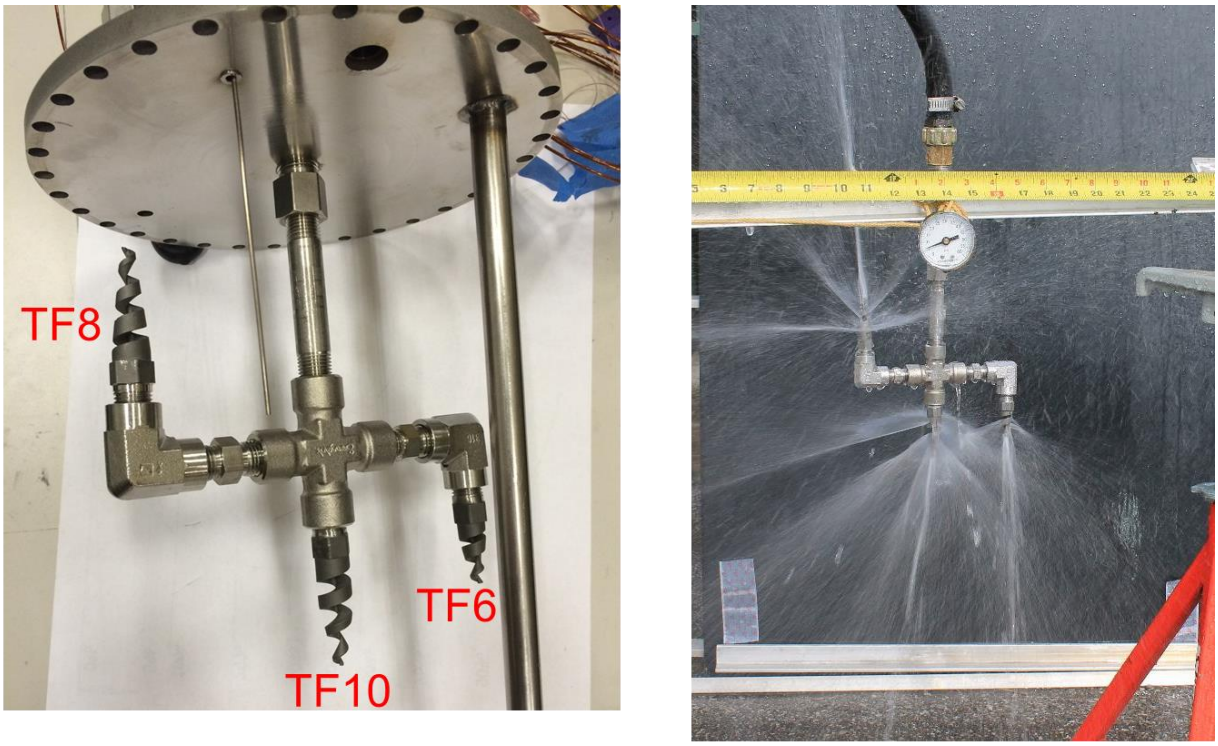

Figure 8: CRYOTE spray injector (left) attached to tank lid, and (right) being tested with water

Given a spray cone with a 170 degree angle, and assuming that the inlet flow has sufficient velocity that its trajectory is nearly a straight line, one can estimate the portion of the tank wall that will be hit by the spray. The upward spray will cover the wall above a height of z = 27.1 inches, at the fill level of 98% (by volume). The downward spray will cover the wall below a height of z = 22.1 inches, the 84% fill level. Approximately 17% of the wall surface area, between the 75% and 92% surface area levels, will not be directly impinged by the spray.

The following figures illustrate some of the measured test data. All data were recorded once per second (1 Hz). Estimated uncertainties are 2 K in temperature measurements and 1 psi in pressure measurements. The test shown is "20161006_3NZL_45psia_TC90=168K", conducted October 6, 2016. The VATA supply tank ullage pressure was 45 psia. Thermocouple TC90 was used to trigger closure of the vent valve, when the measured temperature fell below 168 K. TC90 is located on the outside wall of the tank at the 57.5% fill level.

Figure 9 shows the mass of the CRYOTE receiver tank as measured by load cells. The fill valve is opened at 642 s, but liquid does not begin to accumulate in the tank until approximately 800 s. The data show that 370 lbm of LN2 were accumulated in CRYOTE. The slope of the plot after the vent is closed indicate flow rates in the range 0.13 – 0.26 lbm/s.

Figure 10 shows the pressure measured in the ullage of the VATA supply tank (black line), in the transfer line just upstream of the injector (orange line), and in the ullage of the CRYOTE receiver tank (green line). Note the fluctuations in pressure upstream of the injector during the first ~100 seconds of flow. At 780 seconds, the flow nearly stalls when the receiver tank ullage pressure rises almost to match the supply tank pressure, but the pressure soon falls and the fill is successful. Finally, note the increase in pressure after the vent valve closes at 913 seconds.

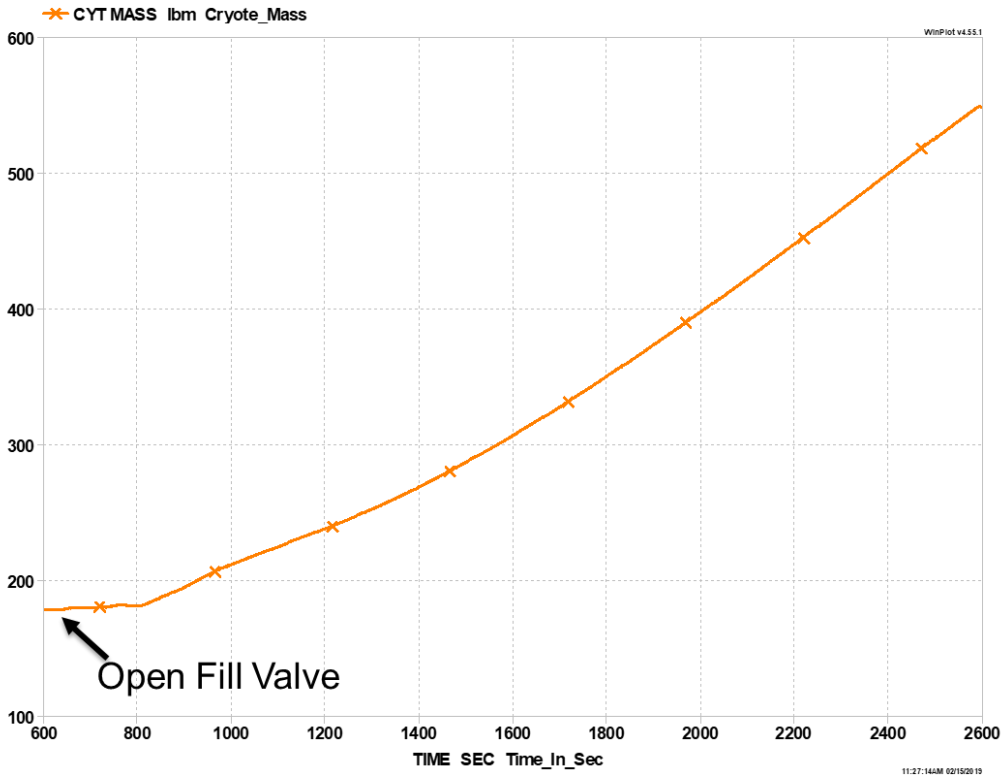

Figure 9: Mass of CRYOTE receiver tank and contents (lbm)

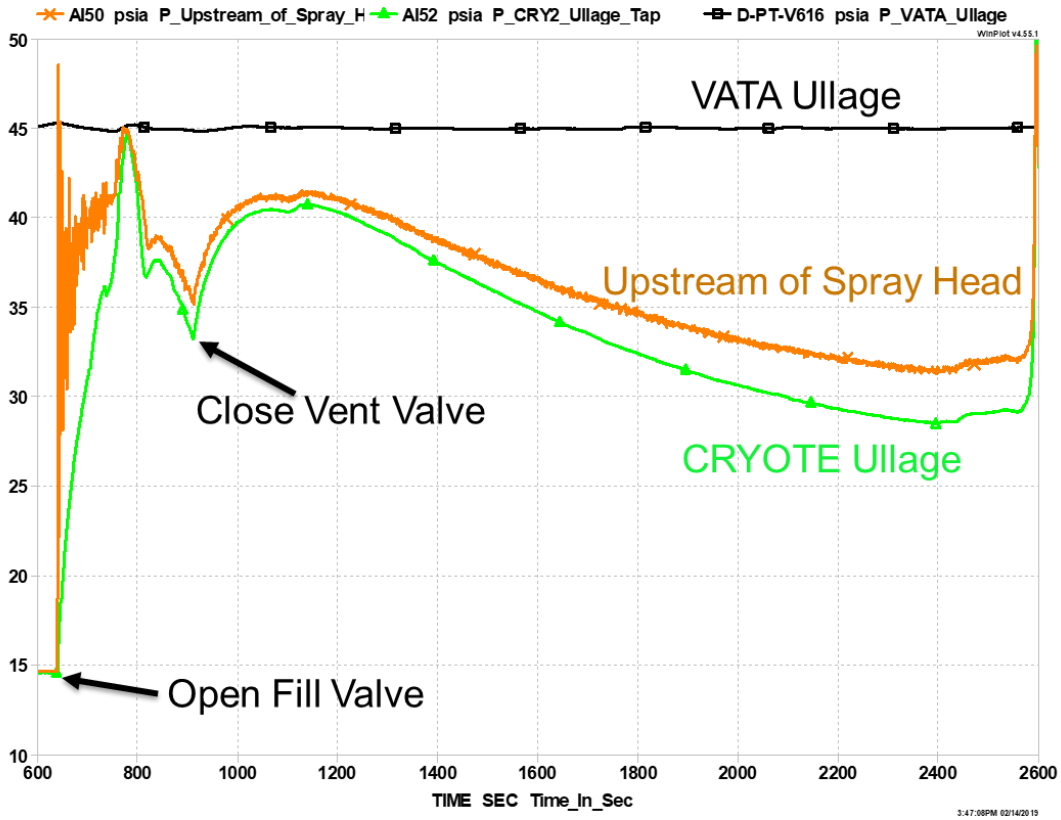

Figure 10: Test system pressures (psia)

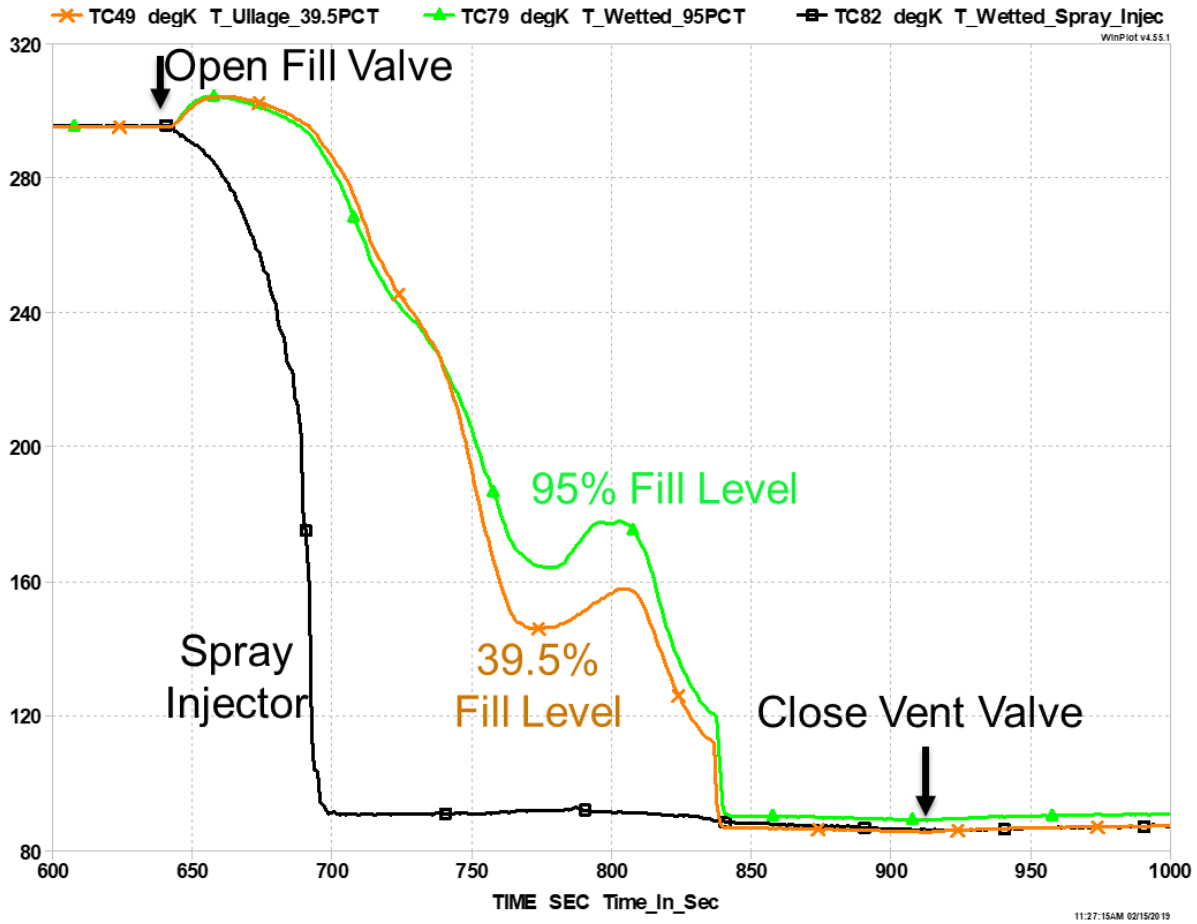

Figure 11: CRYOTE wetted tank temperatures (K)

Figure 11 shows the wetted thermocouple temperature measurements (K) of the spray injector and inside the tank volume at the 39.5% and 95% fill levels. Note the rises in temperature at 650 and 800 seconds corresponding to the increases in pressure shown in Figure 10. By the time the vent valve is closed at 913 seconds, temperatures inside the tank have dropped nearly to saturation. This suggests that internal, wetted thermocouples would not make good triggers for closure of the vent valve.

Figure 12 shows the external wall temperatures (K) of the CRYOTE tank. The titanium wall is 0.05 inches thick. In general, the wall chills more quickly at lower fill levels, but even the 99.3% fill level (orange line) has chilled down long before the tank fills. The vent valve closed when TC90 (purple line) fell below 168 K.

Figure 13 shows the temperatures (K) measured on the outside of CRYOTE's stainless steel lid. Note that the 0.38-inch thick lid is almost eight times thicker than the walls of the titanium sphere, so chilldown times are longer than the wall temperatures shown in Figure 12.

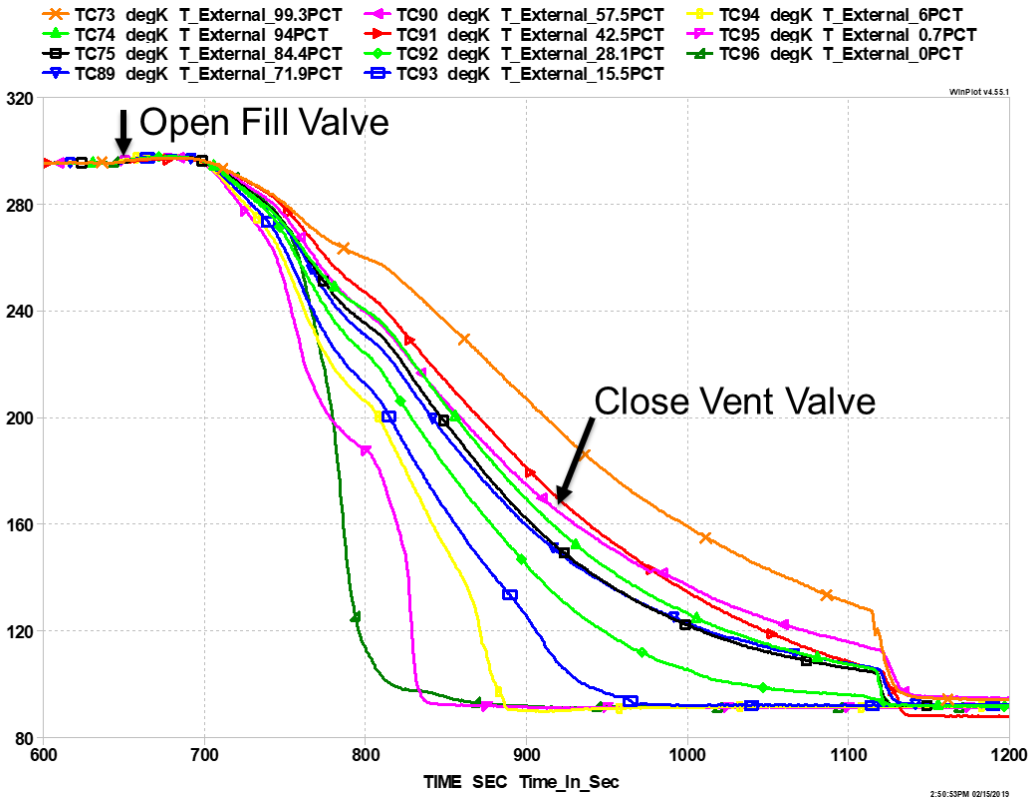

Figure 12: CRYOTE external wall temperatures (K)

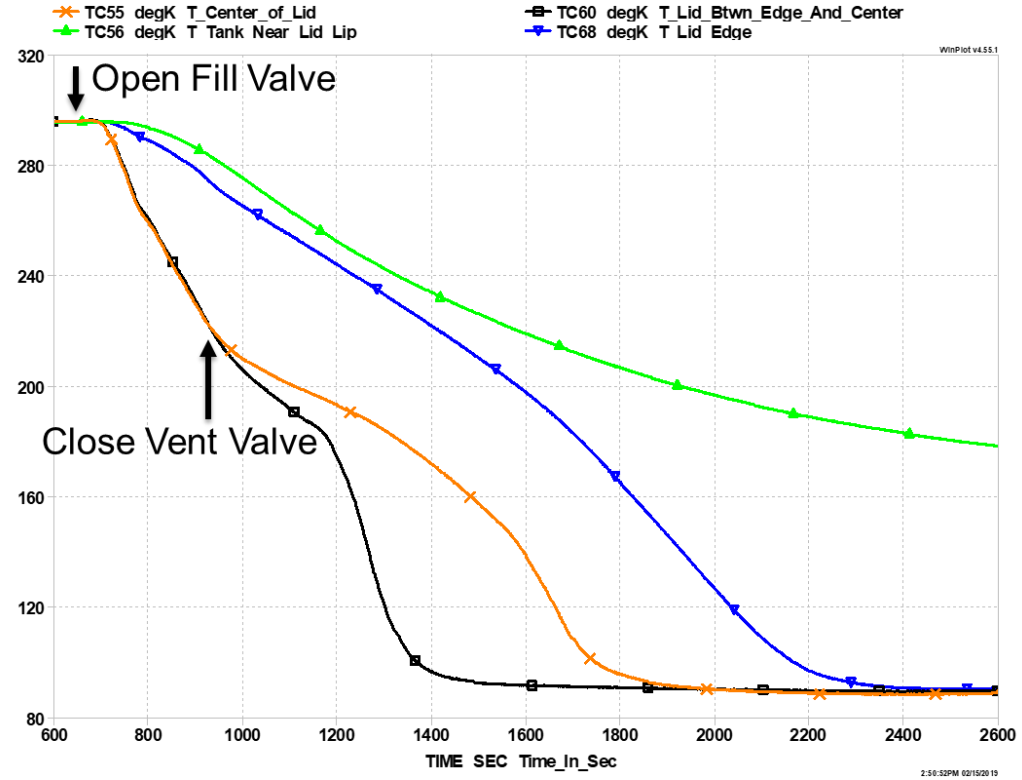

Figure 13: CRYOTE external lid temperatures (K)

IV.GFSSP Model of VCNVF Experiments

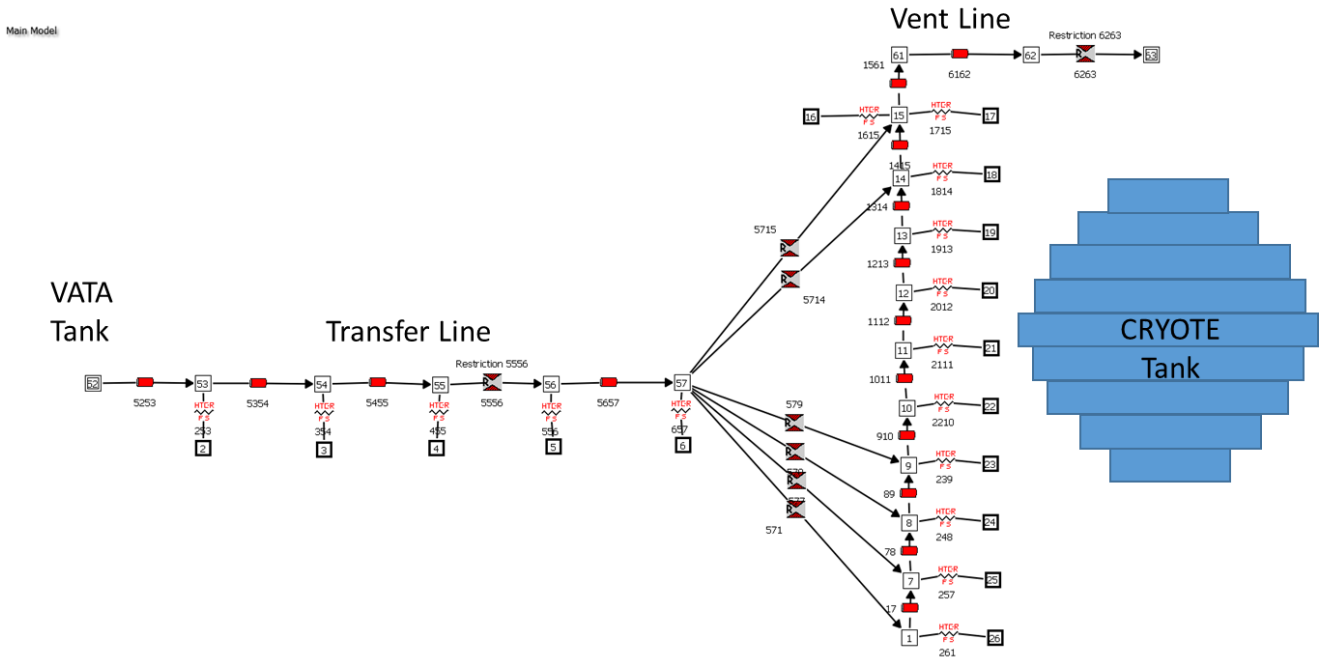

Figure 14. GFSSP Model of CRYOTE tank with inlet and outlet transfer line

The spherical CRYOTE tank was represented by 10 nodes and 9 branches as shown in Figure 14. The tank was modeled as nine vertical, cylindrical pipes of equal length and varying diameters. The height of the tank was divided into nine equal segments that was assigned to the length of each pipe. The diameter of each circular pipe was calculated to ensure that the volume of the cylindrical pipe is equal to the volume of the spherical sector of the same length. The tank's titanium wall was represented by 10 solid nodes (Nodes 17 to 26) of uniform mass. Solid node 16 represented the mass of the stainless steel lid. The heat transfer between the solid to fluid nodes was calculated using the pool boiling correlation described in Section II of this paper.

The spray shown in Figure 8 was represented by six branches with the restriction option (orifice). Two branches (5714 & 5715) represent the upward nozzle and four branches (571,577,578 and 579) represent the downward nozzles.

Node 52 represents the VATA supply tank which was maintained at 45 psia during the test. The transfer line between VATA and the CRYOTE Tank was represented by four circular pipe branches (5253, 5354, 5455 and 5657). The metal wall of the transfer line was represented by five solid nodes (2, 3, 4, 5 and 6). The heat transfer between solid and fluid in the transfer line was calculated using the Miropolskii [16] correlation for film boiling forced convection heat transfer.

The resistance of the inlet valve was set to attain the estimated flowrate range of 0.13-0.26 lbm/sec during tank filling when the vent valve was closed. The vent line was represented by two branches of circular pipe (1561 and 6162) and one branch to represent the vent valve (6263).

V. Results & Discussion

This section describes the modeling results of the VCNVF experiment described in Section III of the paper. The predicted tank pressure, filling of the tank, and chill down of the wall and ullage are compared with the test data. The

predicted flowrate to and from the tank, boiling and condensation heat transfer coefficients, and evaporation are also presented.

Figure 15 shows the comparison of predicted and measured tank pressure history during the chill and fill process. Both the measured and predicted pressure show a rapid rise followed by a fall in pressure due to cooling and condensation. The pressure starts rising again after the closure of the vent valve. After reaching a peak, the pressure starts falling mainly due to condensation of vapor in the tank. Numerical predictions compare reasonably well with the test data. The observed discrepancy in the peak pressure is not much greater than the experimental uncertainty.

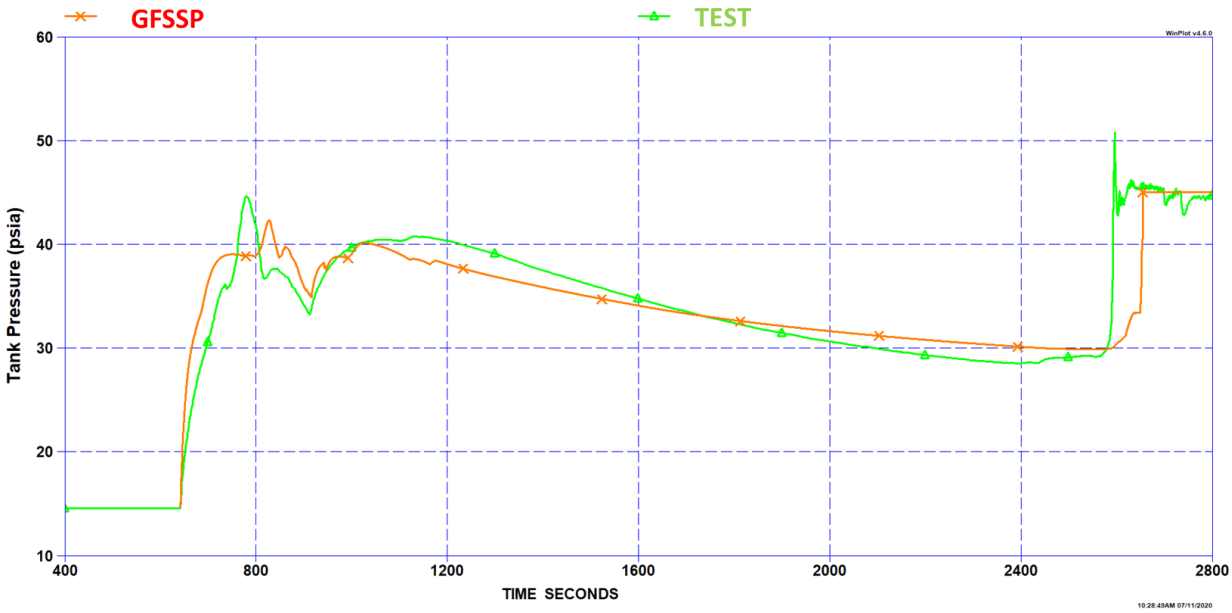

Figure 15. Measured and predicted pressure history during chill and fill of CRYOTE Tank

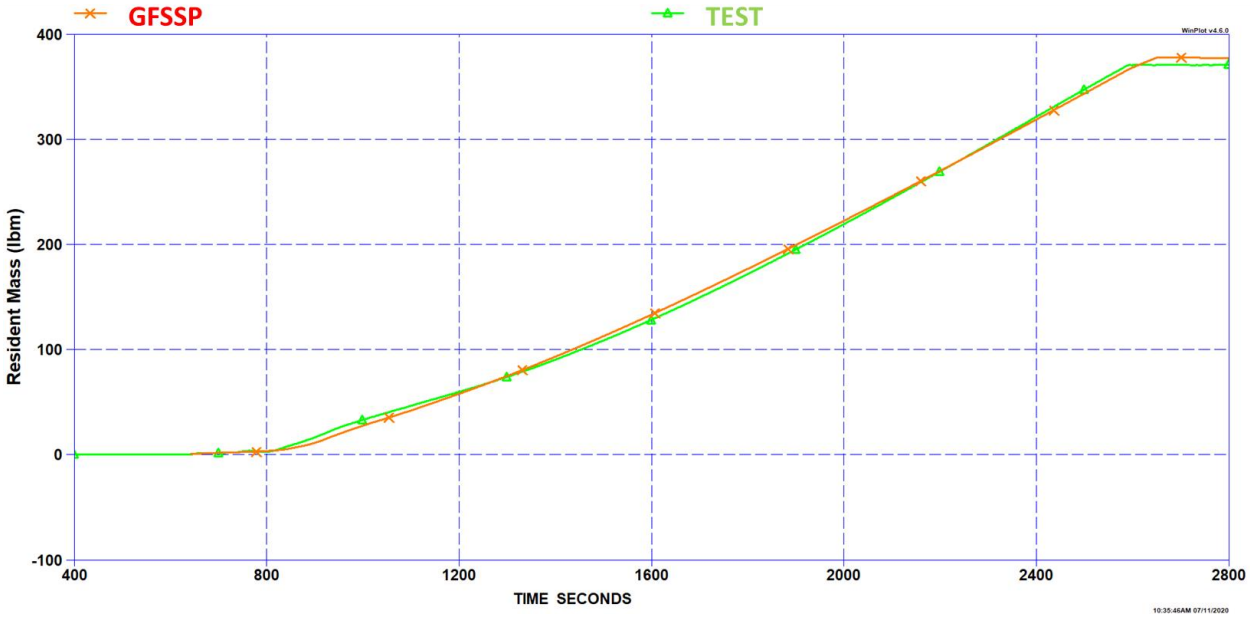

Figure 16. Measured and predicted history of resident mass in the tank during chill and fill

Measured and predicted history of resident mass in the tank during the chill and fill process are shown in Figure 16. Excellent agreement is observed between the measured and test data.

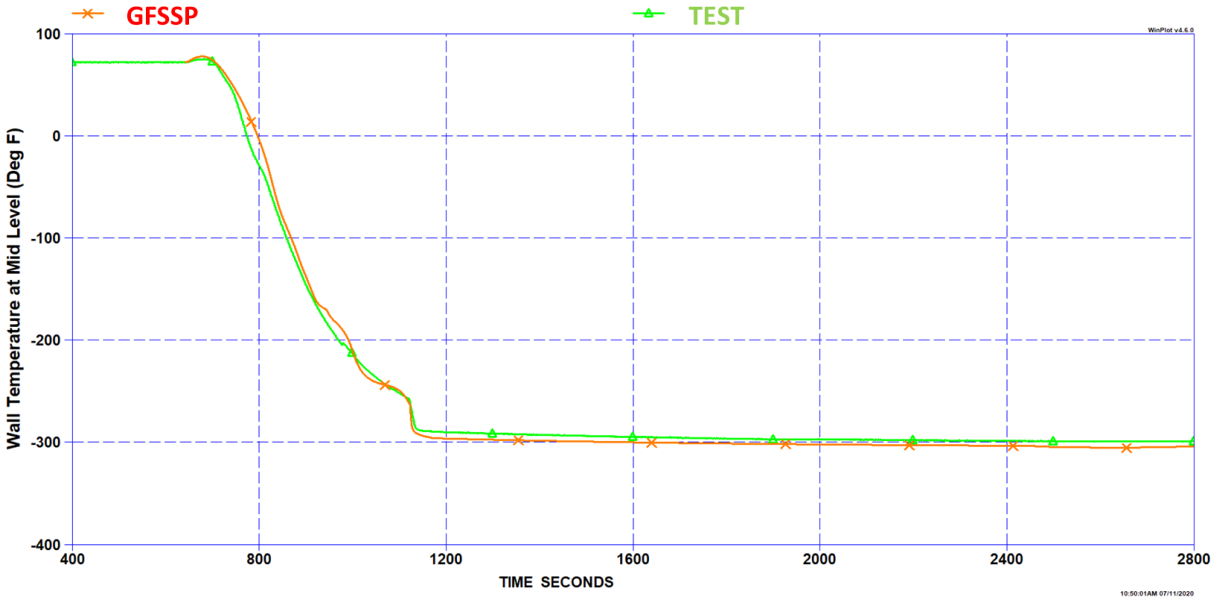

Figure 17. Measured and predicted wall temperature at 57.5% level.

During the test, the vent valve was closed when the temperature sensor (TC90) located at 57.5% level reached 168 K (-157 ˚F). Figure 17 shows the comparison of predicted temperature at 50% level and measured wall temperature at 57.5% level. This demonstrates that the boiling correlation compiled in Reference 9 accurately predicts tank chilldown.

Figure 18 shows the comparison of the predicted ullage temperature at the 50% level with measured ullage temperature at the 39.5% level.

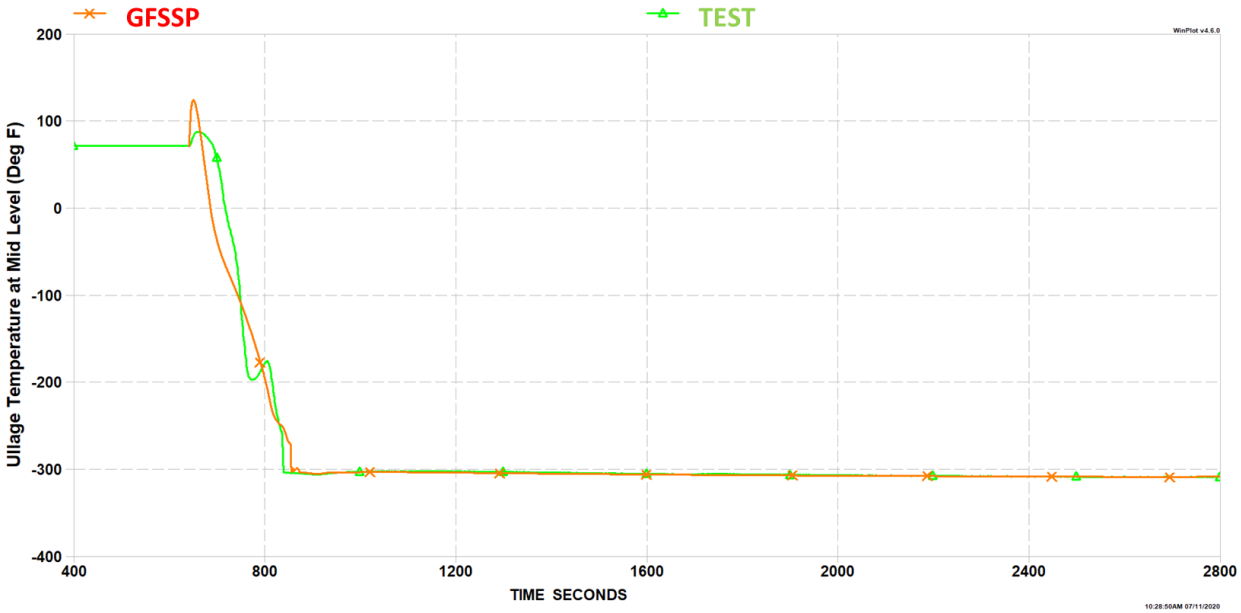

Figure 18. Measured and predicted ullage temperature.

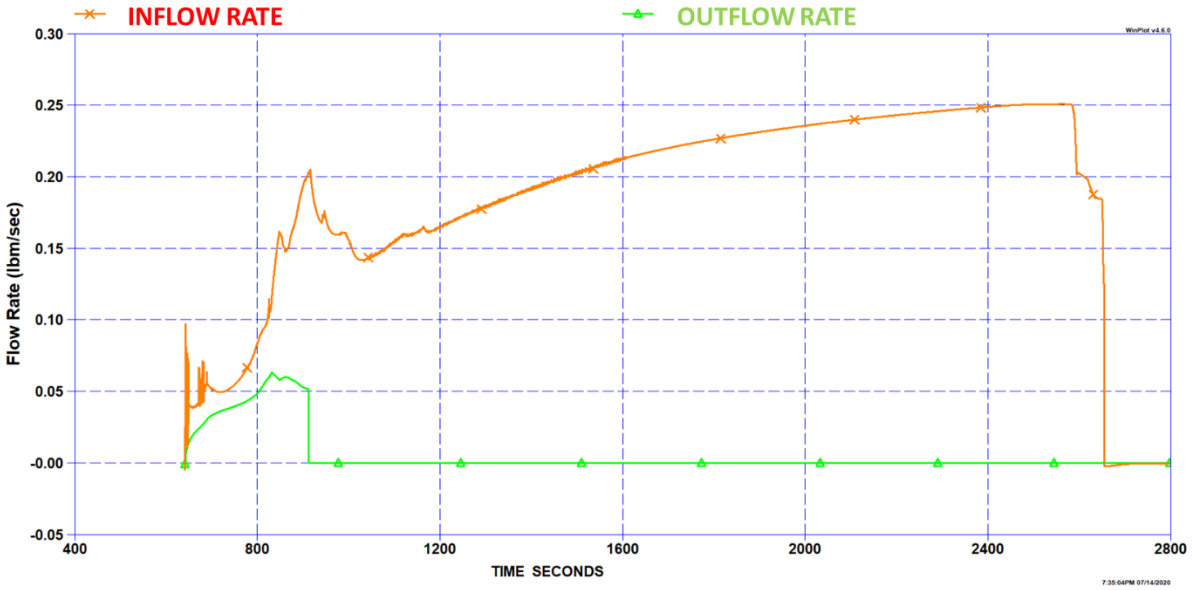

Figure 19. Predicted inflow rate and outflow rate in the Tank

The predicted mass flowrate into the tank and mass flowrate from the tank is shown in Figure 19. Mass flowrate was not measured in the experiment. However, an approximate range of mass flowrate has been estimated from the history of resident mass in Section III. The predicted mass inlet flow rate after vent closure is within the range of 0.13-0.26 lbm/sec estimated from the test data. The outflow rate is zero after 913 seconds when the vent valve is closed.

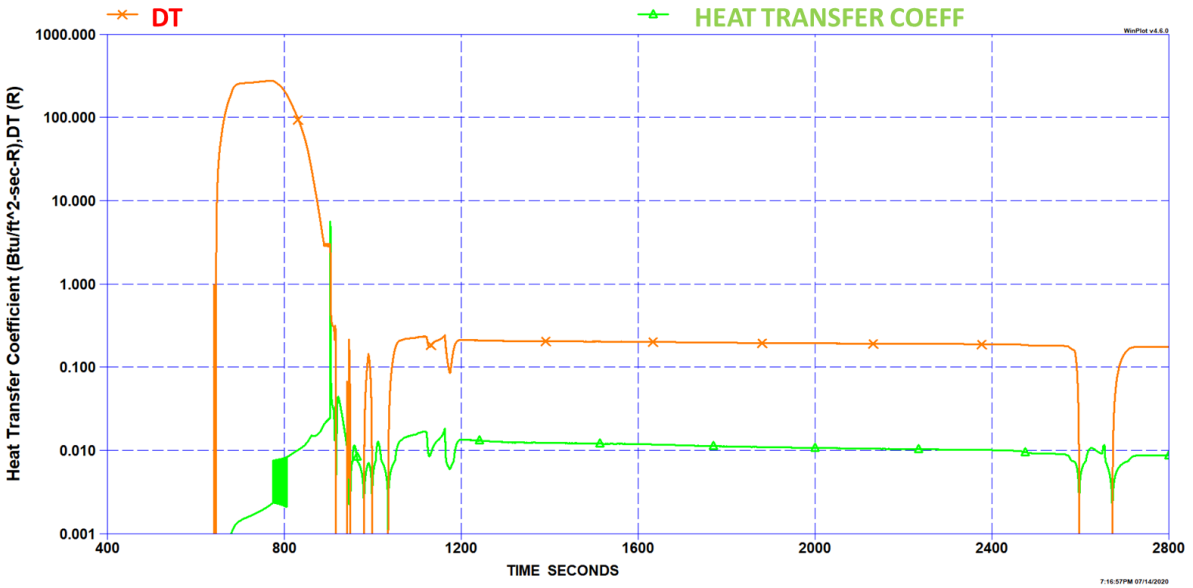

Figure 20. Predicted heat transfer coefficient and corresponding temperature difference between solid and fluid node at the tank bottom

The predicted heat transfer coefficient and temperature difference between solid node and fluid node at the tank bottom is shown in Figure 20. Figure 21 shows the different boiling regimes as the wall is cooled down from ambient temperature to cryogenic temperature.

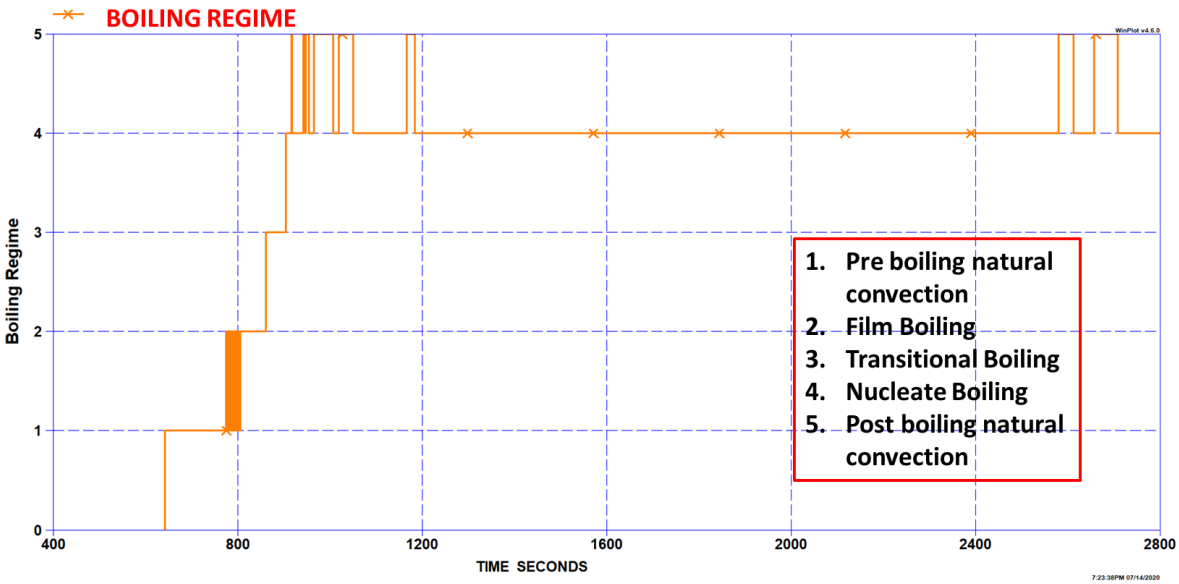

Figure 21. Boiling Regime at the tank bottom

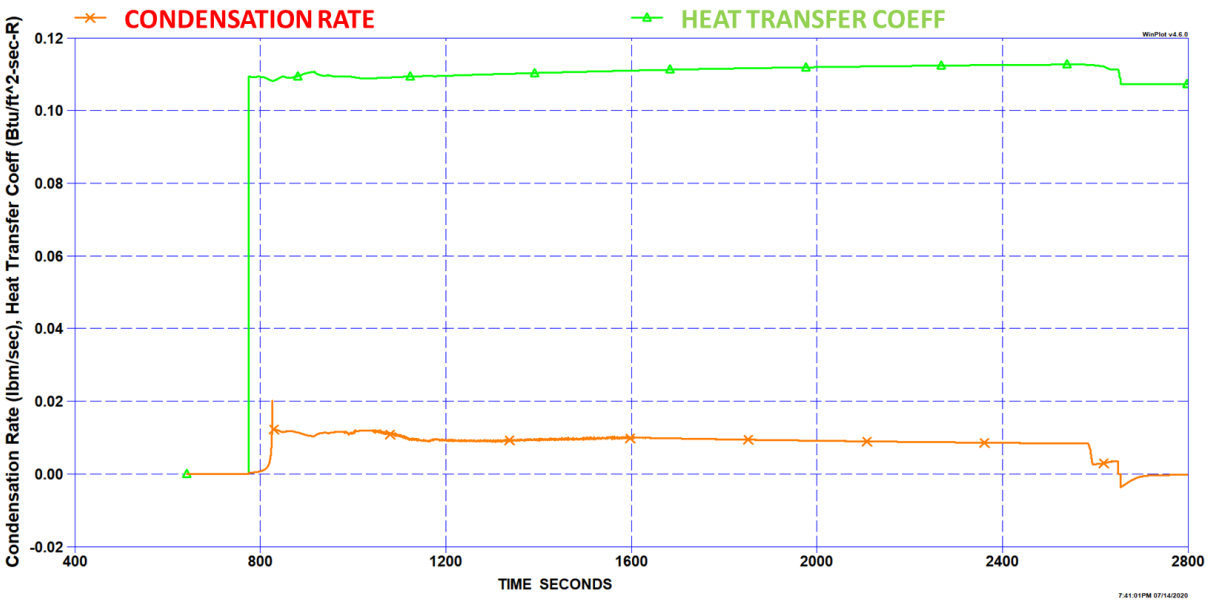

Figure 22. Predicted condensation rate and condensation heat transfer coefficient

Figure 22 shows the predicted condensation rate and condensation heat transfer coefficient during the chilldown process. It may be noted that condensation starts only when vapor reaches saturation temperature.

VI. Conclusions

This paper demonstrates that it is possible to simulate chilldown and filling of a cryogenic tank using GFSSP, a general purpose flow network code based on a finite volume procedure of solving the mass, momentum, and energy conservation equations for a thermo-fluid system. For accurate modeling of tank chilldown, it is necessary to calculate heat transfer from solid to fluid using boiling correlations which include film, transition, and nucleate boiling, as well as natural convection during pre- and post-boiling. It is also necessary to account for the condensation of vapor in the

tank when it comes into contact with the liquid spray. More work is needed to develop a generalized condensation model which is applicable for a wide variety of spray nozzles.

Acknowledgments

This work has been supported by Reduced Gravity Cryogenic Transfer (RGCT) project managed by NASA/Glenn Research Center. The authors would like to acknowledge Professor Mostafa Ghiaasiaan of the Georgia Institute of Technology for his suggestions and review of the condensation model during the course of this work.

References

1. David Chato & Rafael Sanabria, "Review and Test of Chilldown Methods for Space-Based Cryogenic Tanks", NASA Technical Memorandum 104458, AIAA-91-1843.
2. Rhys, Noah, "Vented Chill / No-Vent Fill Experiments on a 30-inch Diameter Tank using LN2" Presentation in ER24 Propulsion Research & Technology Branch, December, 2014.
3. Generalized Fluid System Simulation Program, Version 6.0, User Manual, March 2016, NASA/TP-2016-218218.
4. LeClair, Andre and Majumdar, Alok, "Computation Model of the Chilldown and Propellant Loading of the Space Shuttle External Tank", Paper No. AIAA 2010-6561, 46th AIAA/ASME/SAE/ASEE Joint Propulsion Conference & Exhibit, 25-28 July, 2010.
5. Alok Majumdar, "No Vent Tank Fill and Transfer Line Chilldown Analysis by GFSSP", presented in Thermal & Fluids Analysis Workshop (TFAWS 2013), July 29 – August 2, 2013, Kennedy Space Center, Florida.
6. Alok Majumdar, "A Finite Volume Procedure for Thermofluid System Analysis in a Flow Network" p 231-265, 50 Years of CFD in Engineering Sciences, A Commemorative Volume in Memory of D. Brian Spalding, Springer, 2020.
7. Patankar, S. V., "Numerical Heat Transfer and Fluid Flow", Hemisphere Publishing Corp., Washington, D. C., 1980.
8. Hendricks, R. C., Baron, A. K., and Peller, I. C., "GASP - A Computer Code for Calculating the Thermodynamic and Transport Properties for Ten Fluids: Parahydrogen, Helium, Neon, Methane, Nitrogen, Carbon Monoxide, Oxygen, Fluorine, Argon, and Carbon Dioxide", NASA TN D-7808, February, 1975.
9. Hartwig, Jason, Unpublished work on Liquid Nitrogen Pool Boiling Heat Transfer Correlation, 2019.
10. Wang Lei, Wang Jiaojiao, Yan Tian, Ye Shixuan, Xie Fushou, Li Yanzhong, "Film Boiling Heat Transfer Prediction of Liquid Nitrogen from Different Geometry Heaters." International Journal of Multiphase Flow, vol. 129, 2020, pp. International journal of multiphase flow, August 2020, Vol.129.
11. Baumeister, K, and F Simon. "Leidenfrost Temperature—Its Correlation for Lipid Metals, Cryogens, Hydrocarbons, and Water." Journal of Heat Transfer, vol. 95, no. 2, 1973, pp. 166–173.
12. Lienhard, J, and V Dhir. "Hydrodynamic Prediction of Peak Pool-Boiling Heat Fluxes from Finite Bodies." Journal of Heat Transfer, vol. 95, no. 2, 1973, pp. 152–158.
13. V.M. Borishansky, B.I. Bodrovich, F.P. Minchenko, "Heat transfer during nucleate boiling of water and ethyl alcohol", published in a volume of collection of articles, in: S.S. Kutateladze (Ed.), Aspects of Heat Transfer and Hydraulics of Two-Phase Mixtures, Govt. Energy Publishing House, Moscow, 1961,pp. 75–93.
14. Y. Shirai, H. Tatsumoto, M. Shiotsu, K. Hata, H. Kobayashi and Y. Naruo, "Boiling heat transfer from a horizontal flat plate in a pool of liquid hydrogen," *Cryogenics*, p. 410–416, 2010.
15. Kronig, R., and Brink, J. C.," On the theory of extraction from falling droplets", Appl. Sci Res., A2, 142-154.
16. Miropolskii, Z. L., "Heat Transfer in Film Boiling of a Steam_Water Mixture in Steam Generating Tubes", Teploenergetika, Vol. 10, No.5, 1963, pp 49-52 (in Russian; translation Atomic Energy Commission, AEC-Tr-6252, 1964).